

A CASE STUDY OF A MIDTROPOSPHERIC COLD VORTEX IN THE SUBTROPICS OF SOUTH AMERICA

Marcelo Seluchi and Prakki Satyamurty
 Centro de Previsão de Tempo e Estudos Climáticos (CPTEC)
 Instituto Nacional de Pesquisas Espaciais (INPE) – Cachoeira Paulista – SP – Brazil.
 Rod. Pte Dutra Km 39, Cachoeira Paulista, SP, (12630-000)
 Seluchi@cptec.inpe.br

RESUMO

Este trabalho descreve a estrutura sinótica-dinâmica de um vórtice de altos níveis sobre latitudes subtropicais da América do Sul. O centro ciclônico formou-se entre duas regiões baroclínicas associadas respectivamente a um sistema frontal e a uma perturbação proveniente do Oceano Pacífico.

Com o objetivo de diagnosticar os processos físicos responsáveis pelo desenvolvimento do vórtice utilizou-se a equação da vorticidade, que foi avaliada com os diagnósticos gerados pelo modelo regional Eta/CPTEC. A advecção horizontal de vorticidade ciclônica e o termo da divergência foram os fatores que mais contribuíram na formação do sistema.

1. INTRODUCTION

Subsynoptic scale cold vortices are sometimes responsible for severe weather. They were observed by Rasmussen and Zick (1987) over the Eastern Mediterranean with the aid of the satellite imagery, and likened to polar lows. Businger and Reed (1989) reviewed the subject of polar lows and their genesis to diagnose common types of development and addressed the problem of forecasting them. They identified three types of low development: short wave/jetstreak type, arctic front type and cold low type. The present study undertakes an analysis of a cold-core upper air vortex observed over the subtropical South America. For a truly satisfactory analysis of the three-dimensional structure of these small synoptic disturbances a dense network of observations is necessary. However, due to the paucity of observations the study is made with the help of the NCEP operational analyses and the GOES-8 satellite IR imagery. The Eta-CPTEC regional model is used to diagnose this event by running it with the real (observed) boundary conditions.

The general characteristics of the upper cold core vortices over the South American subtropics are obtained from the daily weather discussions at CPTEC during the years 1997 through 2000. These vortices are quite distinct, in many respects, from the vortices studied by Kousky and Gan (1981), Whitfield and Lyons (1992) and Ramirez (1999) and the comparative characteristics are listed in Table 1.

Table 1: Comparisons of characteristics of the tropical and the subtropical cold core vortices.

Characteristic	Tropical upper cold core vortices	Subtropical upper cold core vortex
Size (half wavelength) and shape	1000 km in E-W direction More elongated in N-S or NW-SE direction in the SH	800 km, more symmetrical
Maximum cyclonic vorticity and level	$2 \times 10^{-5} \text{ s}^{-1}$ 200 hPa	$5 \times 10^{-5} \text{ s}^{-1}$ 300 hPa
Movement	Stationary or slow east to west irregular migration	Steady west to east (with a slight northward component), 9° longitude per day
Latitudinal position	Equator to 15°S	$20^\circ - 30^\circ\text{S}$
Major mechanism/process for maintenance	Advection of planetary vorticity, release of latent heat, mean available potential energy to perturbation potential energy due to cold air subsidence	Advection of relative vorticity and divergence terms and, perhaps, radiative cooling in the middle troposphere for the formation of cold core
Temperature anomaly	-3.5°C (thickness difference between 300 and 200 hPa levels = 40m)	-6.0°C at 500 hPa
Weather	Convection on the periphery with diurnal maximum in afternoon and early evening hours, precipitation maximum in equator-	Low and middle cloud in the center, light to moderate rain along its path

	ward eastern quadrant and mainly cloudless in the center	
Life cycle	Few days to few weeks, generally dissipates over land	3 days from east of Andes to Rio de Janeiro coast where dissipates
Frequency and seasonal preference	60% of the days in summer (Dec-Jan-Feb in SH) in Tropical Atlantic	4 to 5 episodes in winter (May-Jun-Jul in SH)
Vertical structure	Vorticity and cold anomaly maxima near 200 hPa level, no significant tilt of the vortex in the vertical	Small easterly tilt in vorticity field, vorticity maximum below tropopause and cold anomaly maximum near 500 hPa

2. SYNOPTIC OVERVIEW

a. Synoptic evolution

This section provides a synoptic overview of the atmospheric conditions during the passage and development of the upper level cyclonic vortex that took place between June 12-16. The analysis is based on the NCEP-NCAR six-hourly surface and upper-air gridded reanalyzed field available with a resolution of 2.5° in both latitude and longitude. Additional information including, precipitation fields, aerological soundings and surface data coverage were provided for the June 13-16 period by the Brazilian National Institute of Meteorology (INMET).

On 11 June at 12 UTC a cold front is detected over the eastern coast of South America, which merges with a low-pressure center located over the Atlantic Ocean at 45°S. The 500 hPa circulation is characterized by a large amplitude short-wave disturbance associated with the cold front. Another baroclinic trough penetrates into the continent from the Pacific Ocean, linked to a cold frontal system over the Andes.

On 12 June the former frontal system weakens and becomes almost stationary over the continent north of 20°S. However the humidity contrast is still significant at 850 hPa, and some precipitation appears over subtropical South America. The southernmost cold front approaches 35°S producing cold advection primarily over the Atlantic coast. In the middle and upper troposphere we now recognize a single trough with a strong westward tilt along with two separated jet streams.

During 13 June, as a surface cold core anticyclone penetrates into the continent, both the frontal zones merge into a single baroclinic band. Some precipitation is detected inside the moist and warm air mass near the strong baroclinic region. Middle and upper levels are now characterized by two separate jet streams around a just developed low pressure center and by a warm ridge associated with the surface anticyclone. This cold upper-low exhibits a very small vertical tilt and attains its maximum intensity on 14 June (Fig. 1). During this day some precipitation is found in the northwestern flank of the surface anticyclone, even though the baroclinicity is considerably reduced. The narrow band with strong humidity contrast (panel b) is still present. The temperature distribution at 00 UTC on 14 April shows that the low center at 500 hPa over eastern Paraguay is 5° to 6°C cooler than the surrounding regions, whereas at 250 hPa level it is about 3°C warmer.

On June 15 and 16 the whole upper level low-over-high block tends to decrease in intensity as it gets closer to the Atlantic Ocean. The low-level anticyclone as well as the thickness gradient become weaker and, in spite of that, some light precipitation was found over the eastern coast around 25°S. The upper low-high pressure system is completely dissipated on 17 June.

The Hovmöller diagram of relative vorticity at 500 hPa (Fig. 2) for 25°S shows that the cyclonic perturbation appears over the Pacific Ocean on June 11 and travels with a quasi-uniform speed of approximately 15° of longitude a day. This cyclonic vortex reaches a relative maximum on June 12 just before crossing the Andes (located approximately at 67°W at that latitude), then undergoes a moderate weakening at the lee side and reinforces during the next 2 days. After 12 UTC 15 June the cyclonic disturbance enters the decaying phase. During the whole life cycle this low pressure center is preceded and, specially followed by an anticyclonic perturbation. Negative anomalies of potential temperature at 500 hPa also display a strong positive correlation with relative vorticity (i.e., cyclonic vorticity and low temperatures), which is reversed at 250 hPa level. Hovmöller diagrams of geopotential height at 500 and 250 hPa also expose negative anomalies moving eastward, but some orographic noises (and Gibbs effect) make the interpretations more difficult. Beneath 700 hPa it is not possible to identify a cyclonic perturbation neither in vorticity nor in temperature nor in geopotential height fields.

3. ETA MODEL FEATURES

The Eta/CPTEC, originally developed by Mesinger et al. (1988) and described in Black (1994), is a grid-point hydrostatic model and is operationally used at CPTEC with a horizontal resolution of 40 Km and 38 vertical layers since 1997. It has a comprehensive physical package including a modified version of the Betts-Miller con-

vective parameterization and an explicit scheme for large-scale precipitation. Turbulence is represented by Mellor-Yamada 2.5 scheme in the free atmosphere and Mellor-Yamada 2.0 in the surface layer.

The main feature of this model is the η (Eta) vertical coordinate, also known as step-mountain coordinate since the top of the mountains coincides with the model interfaces forming steps. Because the η coordinate is almost horizontal, it is adequate to study the atmosphere in the vicinity of mountains, especially steep mountains as it diminishes the problems related to the calculations of horizontal derivatives.

Initial conditions are taken from the NCEP analyses and boundary conditions are provided at six hourly intervals by the CPTEC/COLA General Circulation Model (GCM). The global model inputs are at triangular truncation T62 and 28 layers of resolution. Annual climatology of soil moisture, seasonal fields of albedo and weakly mean observed sea surface temperatures are used as initial lower boundary conditions. Operational forecasts are available twice a day up to 60 hours range.

4. MODEL DIAGNOSTICS

The term *upper-level system* refers to pressure systems that are below the tropopause, but above 700 hPa. In a more physical sense, *upper-level* refers to a layer within the troposphere that is not significantly affected by friction. In general there are several techniques to diagnose the physical mechanisms responsible for the development of upper level systems. One of them is the height tendency equation, which may be written in its older form proposed by Bjerknes or in its quasigeostrophic version. However, the upper-level vortex studied in this article is characterized by a very modest height change, discouraging its use because the residuals in the equation may have the same magnitude as the height variations. A similar problem may arise from the vertical motion Omega equation, which explains the extremes of the vertical movement as function of (among others) geopotential tendencies and temperature advection. As previously pointed out the geopotential changes are very small and the temperature is not a variable particularly well simulated by the model. A third option, and the one employed here, is the vorticity equation that in a frictionless atmosphere is as follows:

$$\partial\zeta/\partial t = -\mathbf{V}\cdot\nabla(\zeta+f) - \omega\partial\zeta/\partial p - (\zeta+f)\nabla\cdot\mathbf{V} + \mathbf{k}\cdot(\partial\mathbf{V}/\partial p)\mathbf{x}\nabla\omega \quad (1)$$

where the symbols have the usual meaning.

The model experiment initiated at 00 UTC on 12 June employing analyzed (real) boundary conditions is the best to describe the upper-level vortex life-cycle because it has encompassed all the developing steps and has exhibited a very high skill.

Fig. 3(a) exposes the relative vorticity tendency at 500 hPa between 00 and 12 UTC June 14, obtained from the 48hs Eta-CPTEC forecast. Because the cyclonic vortex attains its maximum intensity at 12 UTC on June 14, this pattern represents the mean vorticity tendency during a 12 hours developing period. The highest cyclonic vorticity rate of change at subtropical latitudes (exceeding $2\times 10^{-9} \text{ s}^{-2}$) is located near the upper level trough (broken contours). Other significant cyclonic tendencies are observed near the Andes Mountains, in connection to the cold front displacement and over a zonal band located at approximately 32°S . The maximum anticyclonic development rate is detected at 62°W westward of the cyclonic eddy.

Figure 3(b) presents the total vorticity change during the same period but obtained as the sum of the right side terms from the vorticity equation. It is possible to note that in general there is a very high similarity between both figures a and b, indicating that the right side terms indeed correctly reproduce the observed vorticity changes and that frictional effects are in fact insignificant. In particular it is possible to identify the cyclonic maximum associated with the upper-level trough and the anticyclonic tendency behind it. Figure 4 shows the individual contribution of each term in the vorticity equation to the vorticity change. From this it is apparent that the most important contributors to the vorticity change are the vorticity advection and the divergence effect. The vertical advection and the tilting terms have a negligible influence. A closer inspection reveals that Figs. 4 (a) and (c) exhibit quite similar pattern with a slight zonal shift. Moreover the extreme of cyclonic vorticity change ahead of the upper-level trough seems to be caused by horizontal advection and the anticyclonic increase at the rear part would be the result of the divergence effect

Figure 5 shows the Hovmöller diagram of the joint effect of the horizontal vorticity advection and the divergence term, obtained from the vorticity equation apply to the Eta-CPTEC forecast.. Compared to Fig. 2 the overall field is noisy. Nevertheless it is possible to identify a very good agreement between these two figures, since the maximum of cyclonic activity begins near 75°W at 00 UTC June 12 and ends approximately between 40° - 45°W on 12 UTC June 15. This cyclonic path is also partly broken at 70° - 65°W at 12 UTC on June 12, when it crosses over the Andes, that is about 6-12 hours earlier than in Fig. 2. Vorticity values in Fig. 5 also have a very good correspondence with Fig. 2, exhibiting a relative maximum just before crossing the Mountains (which is overestimated) and another of $6\times 10^{-5} \text{ s}^{-1}$ at 50° - 55°W at 12 UTC on June 12. Anticyclonic vorticity bands before and after

the low pressure center passage are also reasonably well reproduced. Close similarity between Figs. 2 and 5 means that the life cycle of the upper-level cyclonic vortex was basically dominated by the horizontal advection of vorticity and the divergence effect. A supplementary figure not included revealed that the tilting term was also locally important during some short periods of the temporal evolution.

6. SUMMARY AND DISCUSSION

This paper describes the synoptic-dynamic structure of an upper-level vortex in the subtropics of South America in winter 1999. On 13 June 1999 a cyclonic vortex has formed between two baroclinic zones associated respectively to a decaying quasi-stationary front placed over subtropical South America and to a stronger transient disturbance crossing the Andes at middle latitudes. Middle and upper level circulation are characterized by two separated jet streams around a low-pressure center, north of a warm ridge linked to a surface anticyclone. The cyclonic vortex is apparent above 700 hPa but its maximum intensity is observed just below the tropopause level. Its thermal configuration is distinguished by a cold core structure between 700 hPa and 400 hPa and a warmer center at higher levels close to the tropopause. In spite of the presence of some baroclinicity connected with the upper-level low, it is not large enough to constitute a true hyper-baroclinic zone. However some light and moderate precipitation is reported in the northwestern flank of the surface anticyclone. On 15-16 June the whole upper-level low-over-high block has decreased in intensity as it gets closer to the Atlantic coast and it has completely dissipated on 17 June.

In this work special emphasis has been given to explain the physical mechanisms responsible for upper-level cyclonic disturbance life cycle. Preference has been conferred to model-generated data rather than observations because the internal consistency of model products makes them more suitable to physical analysis. On the other hand the observational network and the data coverage have important limitations over large portions of South America. The model experiment initiated at 00 UTC on 12 June employing analyzed (real) boundary conditions is the best to describe the upper-level vortex life-cycle because it has encompassed all the developing steps and has exhibited a very high skill.

In order to diagnose the physical mechanisms responsible for the upper-level vortex development the vorticity equation in a frictionless atmosphere is employed. The most important contributors to the vorticity change at 500 hPa are (a) the vorticity advection and (b) the divergence effect. Moreover the Hovmöller diagram of relative vorticity constructed just based on the horizontal vorticity advection and the divergence terms reproduces the analyzed vorticity evolution with a very good degree of accuracy. In other words the upper-level cyclonic development is the result of the joint effect of cyclonic advection and divergence effect ahead of the transient trough. The vertical advection has a negligible influence during the whole-analyzed period and the tilting term is just locally important during some short periods of the temporal evolution when some convective clouds are detected.

The results shown in this paper are just applicable to the present case study since this kind of meteorological situation may exhibit some different features depending, among others, on the season of the year, the thermodynamic features and the synoptic evolution. A future work will focus a climatological approach to assess the typical causes, dynamical and thermodynamical structure and evolution of such upper-levels systems over South America.

Acknowledgments

Authors wish to thank Dr. Sin Chan Chou and Mr. Jorge Gomes for their help with the Eta regional model. This research was carried out with the support of the Conselho Nacional de Desenvolvimento Científico e Tecnológico (CNPq) of the Ministério da Ciência e Tecnologia of Brazil for Marcelo E. Seluchi. This work was also partially supported by the Fundação de Amparo à Pesquisa do Estado de São Paulo (FAPESP), São Paulo, Brazil.

References

- Black, T. L., 1994: The new NMC mesoscale eta model: Description and forecasts experiments. *Wea. Forecasting*, **2**, 266-278.
- Blustein, H., 1992: *Synoptic-dynamic meteorology in midlatitudes. Vol. I: Principles of kinematics and dynamics*, Oxford Univ. Press, 431 pp.
- Businger, S., and R. J. Reed, 1989: Cyclogenesis in cold air masses. *Wea. Forecasting*, **4**, 133-156.
- Kousky, V. E., and M. A. Gan, 1981: Upper tropospheric cyclonic vortices in the tropical South Atlantic. *Tellus*, **33**, 538-551.
- Mesinger F., Z. I. Janjic, S. Nickovic, D. Gavrillov, and D.G. Deaven, 1988: The step-mountain coordinate: Model description and performance for cases of Alpine lee cyclogenesis and for a case of Appalachian redevelopment. *Mon. Wea. Rev.*, **116**, 1493-1518.
- Ramirez, M. C. V., *Padrões climáticos dos vórtices ciclônicos em altos níveis no Nordeste do Brasil*. (Climatologi-

cal patterns of the upper air cyclonic vortices in the Northeast Brazil.) M. S. Dissertation, INPE, S. J. Campos, SP, Brazil, 104pp.

Rasmussen, E., and C. Zick, 1987: A subsynoptic vortex over the Mediterranean with some resemblance to polar lows. *Tellus*, **39A**, 408-425.

Satyamurty, P., Ferreira, C. C., and M. A. Gan, 1990: Cyclonic vortices over South America. *Tellus*, **42A**, 194-201.

Whitfield, M. B., and S. W. Lyons, 1992: An upper tropospheric low over Texas during summer. *Wea. Forecasting*, **7**, 89-106.

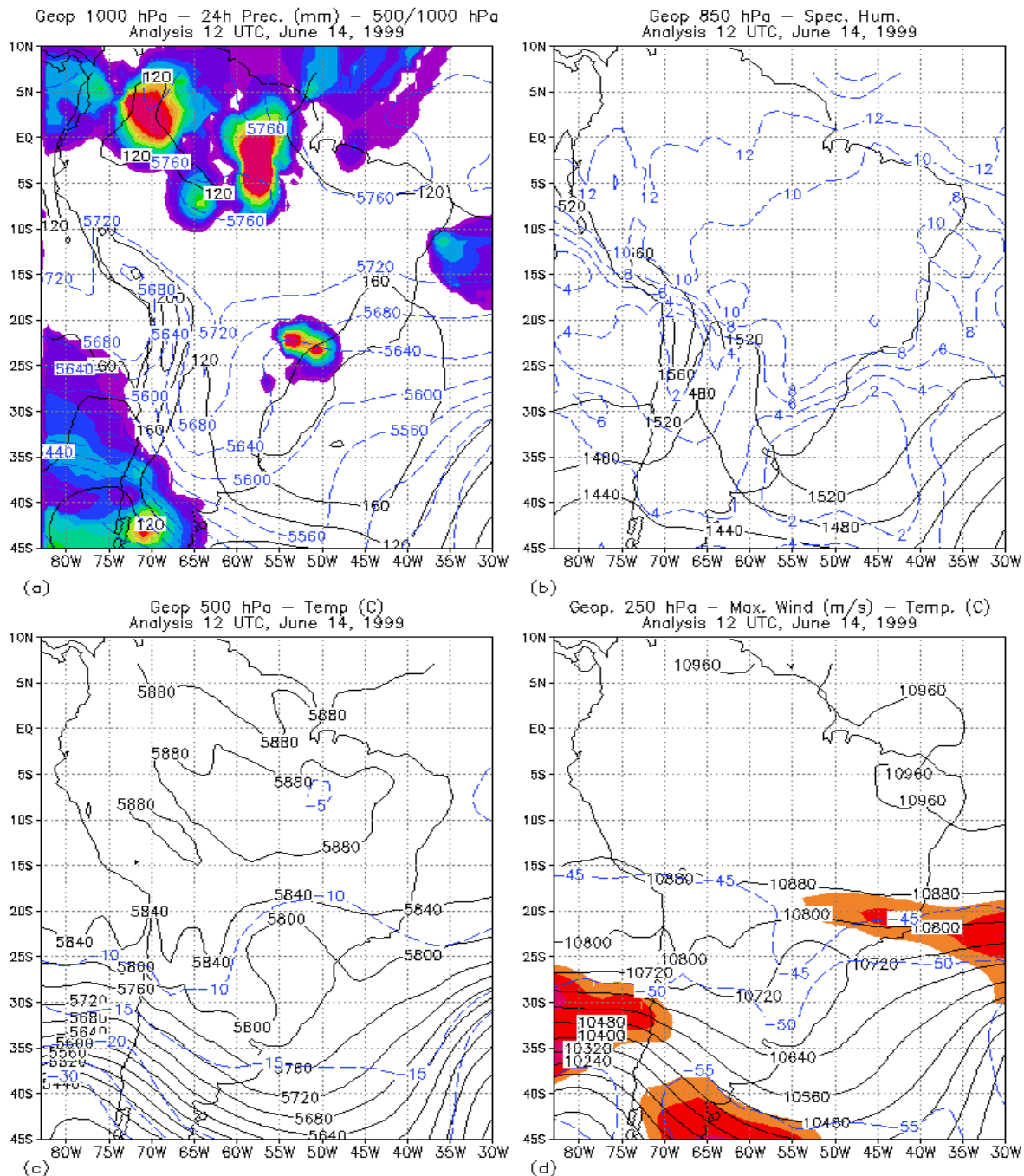


Figure 1: (a) 1000 hPa geopotential height in gpm (solid, negative values are dotted) and 500/1000 hPa thickness in gpm (dashed); (b) geopotential height analysis in gpm (solid) and specific humidity (g/Kg) (dashed) at 850 hPa; (c) geopotential height in gpm (solid) and temperature in C (dashed) at 500 hPa; (d) geopotential height in gpm (solid), temperature in C (dashed) and horizontal wind (values exceeding 40 ms⁻¹ are shaded) for 12 UTC 14 June 1999, (NCEP analysis).

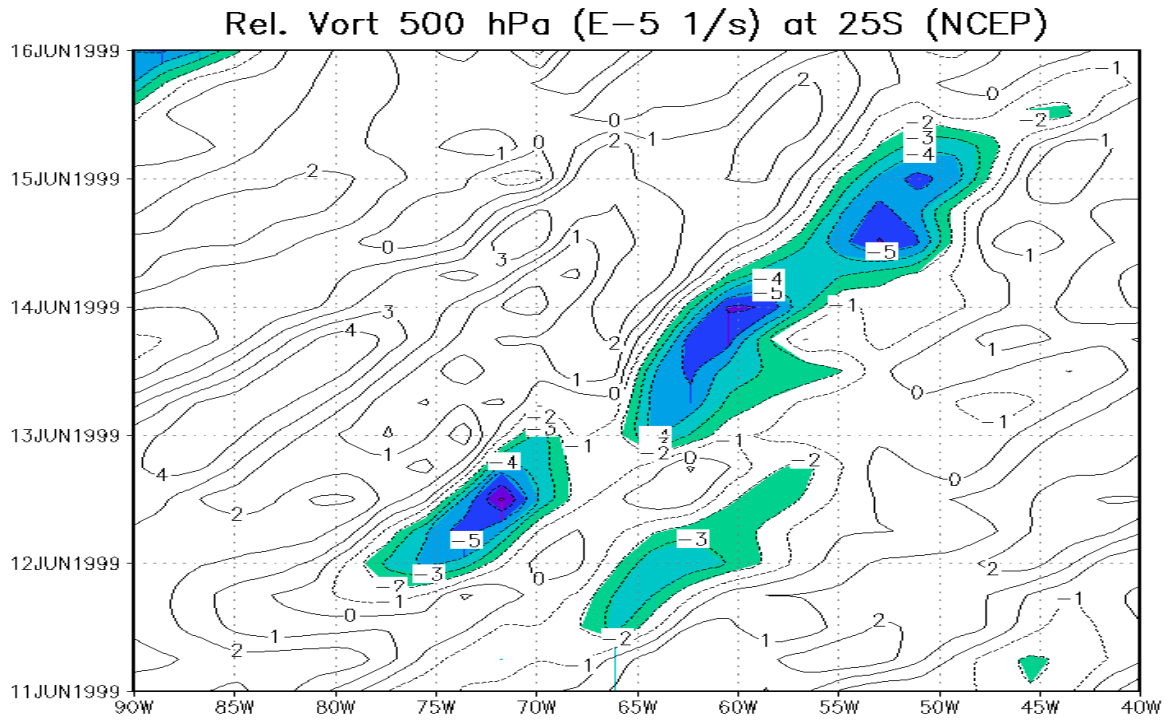


Figure 2: Hovmöller diagram of 500 hPa relative vorticity (10^{-5} s^{-1}) at 25°S (values lower than $-2 \times 10^{-5} \text{ s}^{-1}$ are shaded).

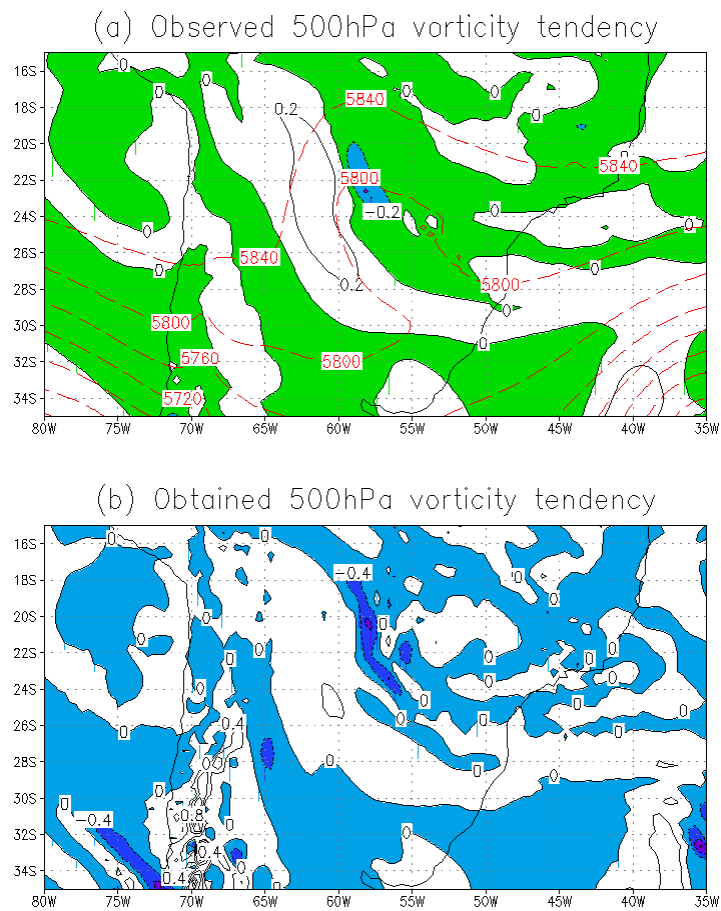


Figure 3: (a) 500 hPa 12 hours tendency of relative vorticity (10^{-8} s^{-2}) between 00 UTC and 12 UTC on 14 June, 1999, dashed lines depict the observed geopotential field (gpm) at 500 hPa; (b) as in (a) but obtained as the sum of the right hand terms from the vorticity equation. Negative values are shaded.

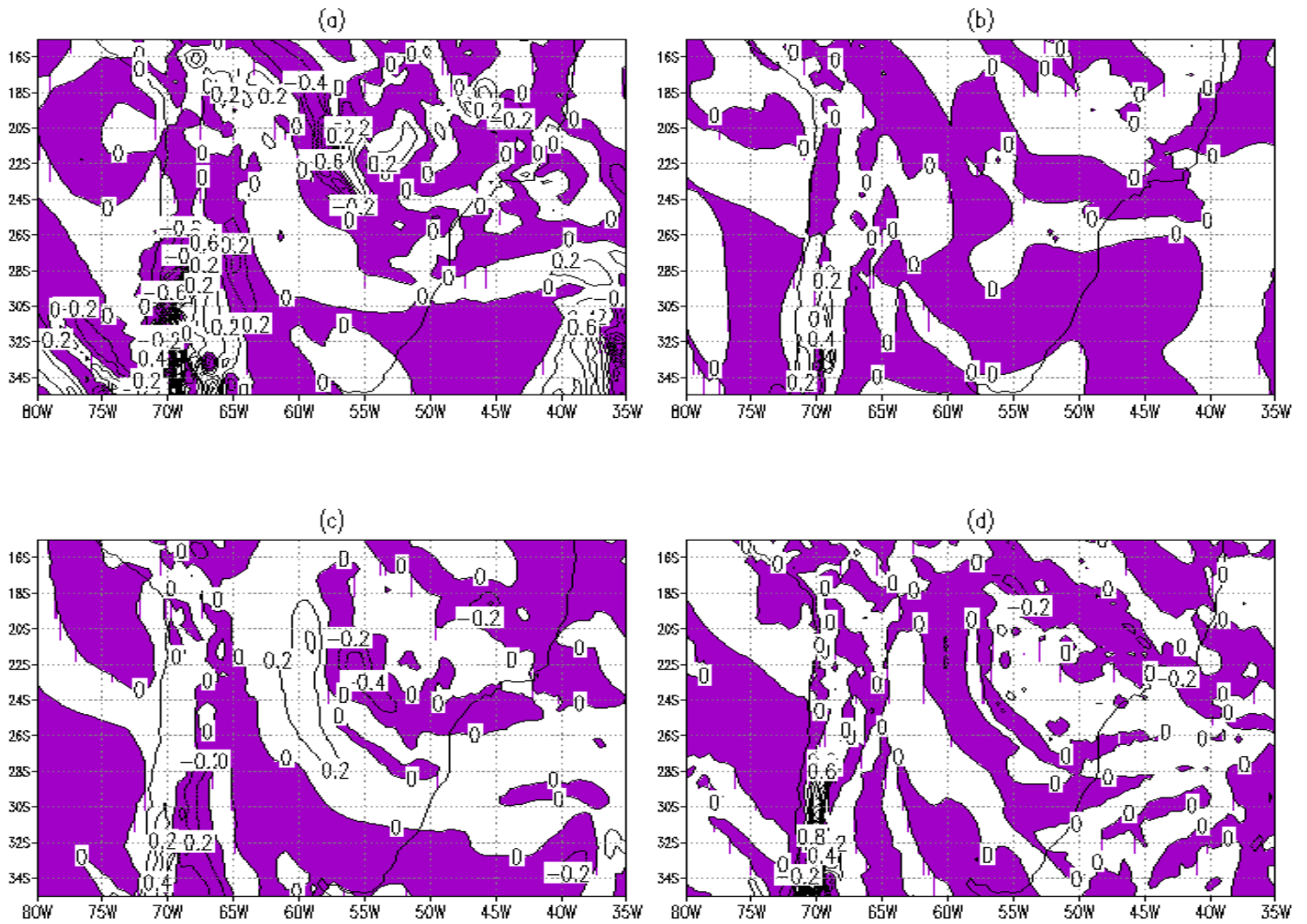


Figure 4: Individual contribution of each term in the vorticity equation to the vorticity tendency (10^{-8} s^{-2}) between 00 UTC and 12 UTC on June 14, 1999. (a) horizontal vorticity advection; (b) vertical vorticity advection; (c) divergence term; (d) tilting term. Negative values are shaded.

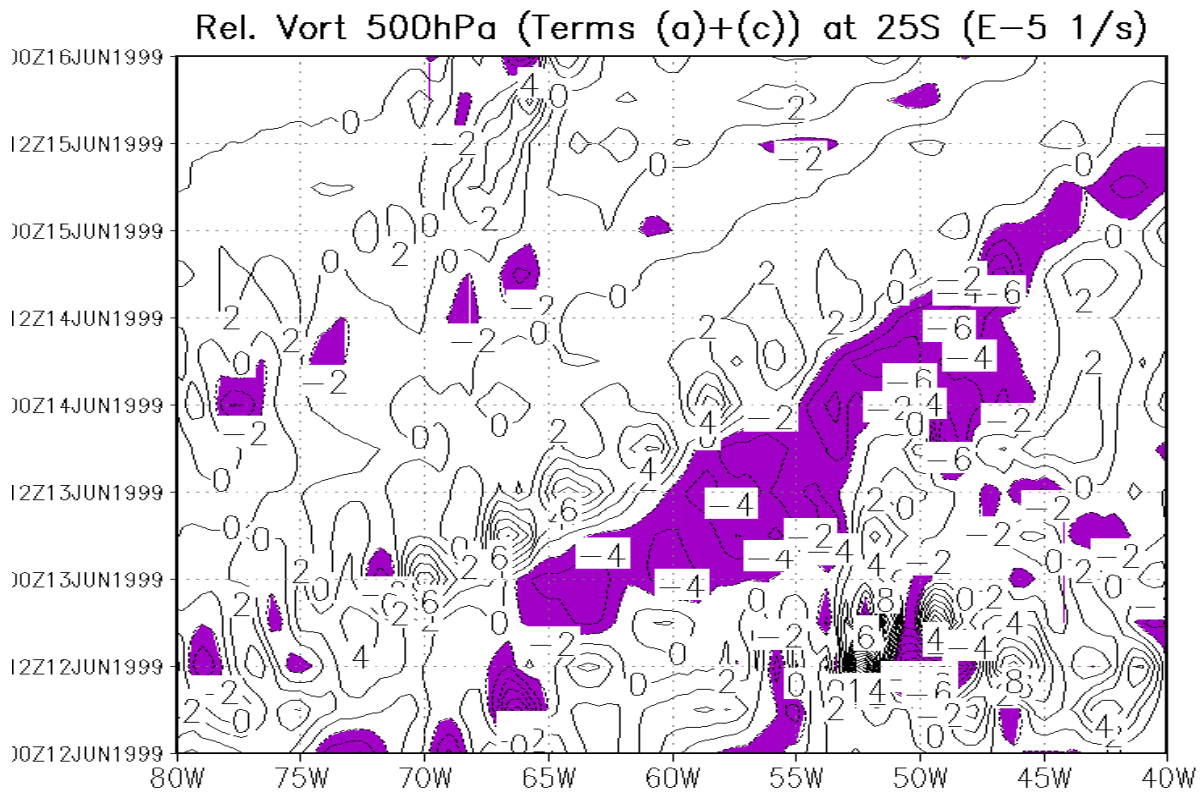


Figure 5: Hovmöller diagram of the joint contributions of terms (a) and (c) in the vorticity equation (10^{-5} s^{-1}) at 25°S (values lower than $-2 \times 10^{-5} \text{ s}^{-1}$ are shaded).